Combined Effects of CO_2 and Light on the N_2-Fixing Cyanobacterium *Trichodesmium* IMS101: A Mechanistic View[1]

Orly Levitan*, Sven A. Kranz, Dina Spungin, Ondřej Prášil, Björn Rost, and Ilana Berman-Frank

The Mina and Everard Goodman Faculty of Life Sciences, Bar Ilan University, Ramat-Gan, 52900 Israel (O.L., D.S., I.B.-F.); Alfred Wegener Institute for Polar and Marine Research, 27570 Bremerhaven, Germany (S.A.K., B.R.); and Laboratory of Photosynthesis, Institute of Microbiology, Academy of Sciences of the Czech Republic, 37981 Třeboň, Czech Republic (O.P.)

The marine diazotrophic cyanobacterium *Trichodesmium* responds to elevated atmospheric CO_2 partial pressure (pCO_2) with higher N_2 fixation and growth rates. To unveil the underlying mechanisms, we examined the combined influence of pCO_2 (150 and 900 μatm) and light (50 and 200 μmol photons m^{-2} s^{-1}) on *Trichodesmium* IMS101. We expand on a complementary study that demonstrated that while elevated pCO_2 enhanced N_2 fixation and growth, oxygen evolution and carbon fixation increased mainly as a response to high light. Here, we investigated changes in the photosynthetic fluorescence parameters of photosystem II, in ratios of the photosynthetic units (photosystem I:photosystem II), and in the pool sizes of key proteins involved in the fixation of carbon and nitrogen as well as their subsequent assimilation. We show that the combined elevation in pCO_2 and light controlled the operation of the CO_2-concentrating mechanism and enhanced protein activity without increasing their pool size. Moreover, elevated pCO_2 and high light decreased the amounts of several key proteins (NifH, PsbA, and PsaC), while amounts of AtpB and RbcL did not significantly change. Reduced investment in protein biosynthesis, without notably changing photosynthetic fluxes, could free up energy that can be reallocated to increase N_2 fixation and growth at elevated pCO_2 and light. We suggest that changes in the redox state of the photosynthetic electron transport chain and posttranslational regulation of key proteins mediate the high flexibility in resources and energy allocation in *Trichodesmium*. This strategy should enable *Trichodesmium* to flourish in future surface oceans characterized by elevated pCO_2, higher temperatures, and high light.

The marine filamentous N_2-fixing (diazotrophic) cyanobacteria *Trichodesmium* spp. bloom extensively in the oligotrophic subtropical and tropical oceans (Carpenter and Capone, 2008). *Trichodesmium* contributes 25% to 50% of the estimated rates of N_2 fixation in these areas, where the new nitrogen inputs stimulate carbon and nitrogen cycling (Capone and Subramaniam, 2005; Mahaffey et al., 2005). The increases in atmospheric CO_2 partial pressure (pCO_2) and the subsequent impacts on ocean acidification are predicted to influence diazotrophs and specifically *Trichodesmium*.

The reported sensitivity of *Trichodesmium* to changes in pCO_2 prompted further investigation into the cellular responses and underlying mechanisms, specifically when combined with other environmental parameters such as temperature, nutrient availability, and light. Elevated pCO_2 significantly increased growth and N_2 fixation rates of *Trichodesmium* cultures (Barcelos é Ramos et al., 2007; Hutchins et al., 2007; Levitan et al., 2007, 2010). The physiological response was also characterized by changes in inorganic carbon acquisition, limited flexibility of carbon-nitrogen ratios, and conservation of photosynthetic activities with increased pCO_2. These manifestations suggested that ATP and reductants [ferredoxin, NAD(P)H] are reallocated in the cells (Levitan et al., 2007, 2010; Kranz et al., 2009, 2010).

In *Trichodesmium*, as in all cyanobacteria, the metabolic pathways of respiration and photosynthesis share several cellular complexes/proteins such as the plastoquinone (PQ) pool, succinate dehydrogenase, and ferredoxin (Fig. 1; Kana, 1993; Bergman et al., 1997; Lin et al., 1998). Energetic currencies [reduced ferredoxin, ATP, NAD(P)H] are also shared and can be allocated and utilized according to cellular requirements. N_2 fixation by nitrogenase and the subsequent

[1] This work was supported by a Reiger Fellowship for Environmental Studies, the Deutscher Akademischer Austausch Dienst, and an Eshkol Fellowship from the Israeli Ministry of Science to O.L., by the European Research Council under the European Community's Seventh Framework Program (FP7/2007–2013)/ERC grant agreement (205150; to B.R.), by the Czech Science Foundation-Grantová agentura České republiky (grant nos. 206/08/1683 and AV0Z50200510 to O.P.), and by the Bundesministerium für Bildung und Forschung-Ministry of Science, Culture and Sport (grant no. GR1950 to I.B.-F.).

* Corresponding author; e-mail levitao@mail.biu.ac.il.

The author responsible for distribution of materials integral to the findings presented in this article in accordance with the policy described in the Instructions for Authors (www.plantphysiol.org) is: Orly Levitan (levitao@mail.biu.ac.il).

www.plantphysiol.org/cgi/doi/10.1104/pp.110.159285

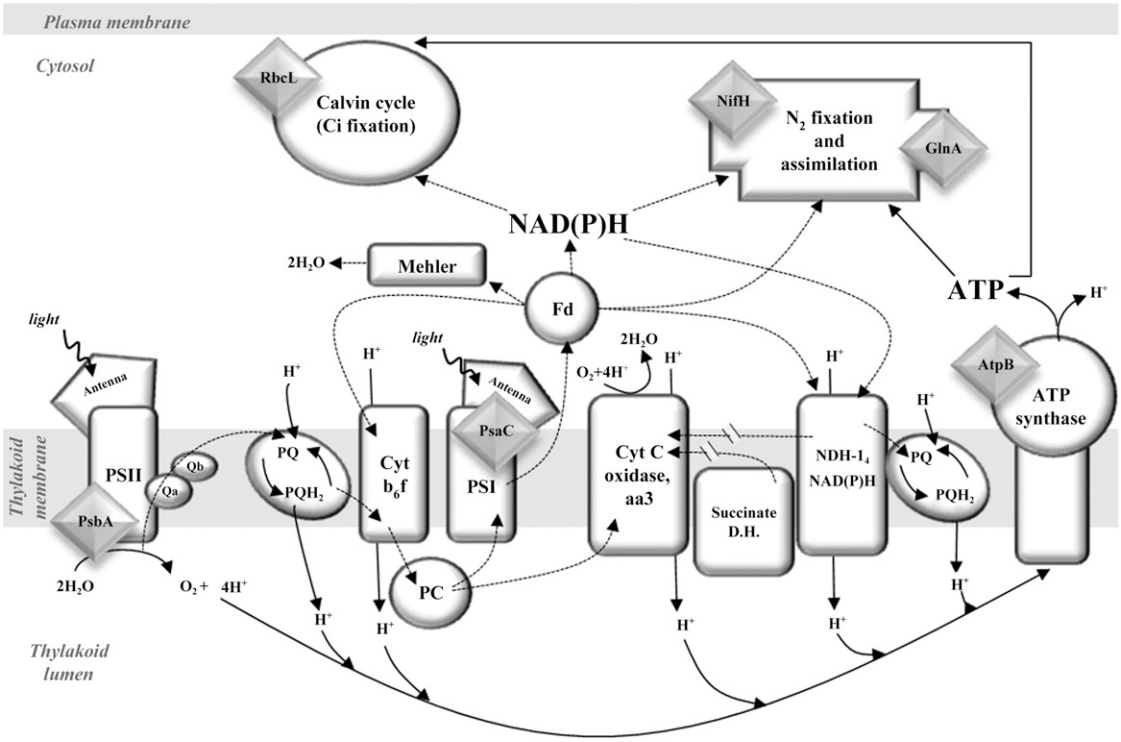

Figure 1. Schematic representation of major cellular complexes involved in energy flow [electron, ATP, NAD(P)H, carbon skeletons] in *Trichodesmium* IMS101. Dashed arrows represent movement direction of electrons, and solid arrows represent directions of protons, ATP, and NAD(P)H. Measured protein subunits are represented by gray diamonds. See Kranz et al. (2010) for measurements of O_2 evolution, inorganic carbon fixation, and fluxes of N_2 fixation.

assimilation of NH_4^+ by Gln synthetase requires carbon skeletons from the tricarboxylic acid reactions. Moreover, linear and pseudocyclic photosynthesis can also generate additional ATP and reductants essential for N_2 fixation (Fig. 1; Berman-Frank et al., 2001).

To understand the regulation of these metabolic pathways in *Trichodesmium* under varying pCO_2 levels and light intensities, we designed an experiment to characterize changes in the fluxes of carbon, nitrogen, and oxygen (O_2), related protein pool sizes, and variable fluorescence parameters of PSII. Elevated atmospheric pCO_2 combined with enhanced sea surface temperatures are forecast to stabilize thermal stratification, resulting in a shallower, more acidified, upper mixed layer characterized by higher mean light intensities (Doney, 2006). Thus, *Trichodesmium* IMS101 cultures were acclimated to past and future pCO_2 levels (150 and 900 μatm) at low and high light (50 and 200 μmol photons m^{-2} s^{-1}).

In the first part of this combined report (Kranz et al., 2010), we examined the physiological responses to the different acclimation conditions. The combination of elevated pCO_2 and light enhanced the production of particulate organic carbon and nitrogen (270% and 390% increase, respectively) as well as growth rates (180% increase; percentages are calculated from Kranz et al., 2010). Generally, the pCO_2-dependent stimulation was higher in cultures acclimated to low light. The pCO_2 effect was also reflected in other measured physiological parameters, particularly the diel patterns of N_2 fixation and the integrated N_2 fixation rates during the day, which increased approximately 30-fold between the low-pCO_2/low-light and the high-pCO_2/high-light acclimations (Kranz et al., 2010). While at high light, elevated pCO_2 extended the period of high N_2 fixation, which lasted from 5 h after the onset of light throughout the end of the photoperiod, the high-pCO_2 contribution to the integrated N_2 fixation was more significant at low light (Kranz et al., 2010). Light, but not pCO_2, influenced gross photosynthesis as measured by PSII O_2 evolution, which increased by approximately 250% in high-light-acclimated cultures. To supply the Calvin cycle with sufficient CO_2, *Trichodesmium* possesses a CO_2-concentrating mechanism mainly based on HCO_3^- uptake (Kranz et al., 2009, 2010). When *Trichodesmium* was acclimated to elevated pCO_2 (900 μatm), a decline in the cellular affinity to dissolved inorganic carbon was observed (Kranz et al., 2009), while the specific uptake of CO_2 showed a 9-fold increase between the low-pCO_2/low-light and the high-pCO_2/high-light acclimations (Kranz et al., 2010).

Proteins are fundamental cellular components that influence the underlying mechanisms subsequently reflected in the cells' physiology. In this study, we extend the experimental results presented by Kranz et al. (2010) by examining the influence of pCO_2 at different light regimes on the photosynthetic fluores-

cence parameters of PSII and on the pool sizes of key proteins involved in carbon and nitrogen fixation and their subsequent assimilation processes.

RESULTS

We quantified amounts of key protein subunits involved in N_2 fixation and assimilation, energy production, and photosynthesis: NifH (iron [Fe] protein of nitrogenase), GlnA (a subunit of Gln synthetase), PsbA (D1 protein of PSII), PsaC (core subunit of PSI), AtpB (the CF_1 subunit of ATP synthase), and RbcL (the large subunit of Rubisco). The amounts (pmol μg protein^{-1}) of these proteins at the two sampling points (1 and 5 h after the onset of light) are presented in Table I. All protein subunits are normalized to total protein amounts. The amount of total protein per cell was similar for all acclimations measured (one-way ANOVA; $P < 0.05$; Scheffe posthoc test; $n = 6$; data not shown). For the two extreme acclimations, the protein amounts were 8.36 ng cell^{-1} for the low-pCO_2/low-light acclimation and 8.23 ng cell^{-1} for the high-pCO_2/high-light acclimation.

Nitrogen Fixation and Assimilation Proteins

The Fe protein subunit of nitrogenase (NifH) was influenced by pCO_2 and time (Fig. 2; Table I). Although light itself did not distinctly influence NifH amounts, the interactions of pCO_2 and light significantly affected the protein pool size. For all treatments, excluding high pCO_2/high light, NifH amounts were higher at 5 h after the onset of light relative to 1 h after the onset of light. At low light (50 μmol photons m^{-2} s^{-1}), pCO_2 concentrations (150 and 900 μatm) did not influence the amount of NifH. At high light (200 μmol photons m^{-2} s^{-1}), high pCO_2 significantly influenced both the amount and the pattern of NifH abundance. NifH amounts remained constant for both time points measured (0.173 $\pm$ 0.025 and 0.167 $\pm$ 0.025 pmol μg protein^{-1}) and were as low as the NifH amounts measured 1 h after light for both low-light acclimations (Fig. 2; Table I). Low-pCO_2/high-light-acclimated cultures had high NifH protein amounts (0.302 $\pm$ 0.068 pmol μg protein^{-1}), which differed from all other treatments (0.169 $\pm$ 0.033–0.217 $\pm$ 0.072 pmol μg protein^{-1}).

NH_4^+ produced by the nitrogenase is incorporated into an organic compound via the GlnA decamer, Gln synthetase (Fig. 1). While both pCO_2 and light affected GlnA amounts, the low-pCO_2/high-light acclimation had the highest GlnA amounts (0.134 $\pm$ 0.007 pmol μg protein^{-1}) of all other acclimations (0.093 $\pm$ 0.005 to 0.116 $\pm$ 0.006 pmol μg protein^{-1}), which paralleled the high amounts of NifH under the same acclimation (Fig. 2; Table I).

ATP Synthase Abundance

AtpB, the CF_1 subunit of ATP synthase, was influenced by neither pCO_2 nor light (Table I). Time de-

Table I. *Average amounts (pmol μg protein^{-1}) of all measured protein subunits in Trichodesmium IMS101*

Shown are results (as averages) for 1 h and 5 h after the onset of light ($n = 3$). Average values of the two sampling points ($n = 6$) are also shown. The proteins measured were PsbA (D1 protein of PSII), PsaC (core subunit of PSI), RbcL (the large subunit of Rubisco), NifH (Fe protein of nitrogenase), and GlnA (a subunit of Gln synthetase).

Protein Amount	50 μmol Photons m^{-2} s^{-1}		200 μmol Photons m^{-2} s^{-1}	
	150 μatm pCO_2	900 μatm pCO_2	150 μatm pCO_2	900 μatm pCO_2
1 h after the onset of light				
PsbA	0.083 $\pm$ 0.022	0.065 $\pm$ 0.021	0.061 $\pm$ 0.010	0.040 $\pm$ 0.000
PsaC	0.113 $\pm$ 0.010	0.136 $\pm$ 0.010	0.098 $\pm$ 0.014	0.092 $\pm$ 0.016
RbcL	0.504 $\pm$ 0.059	0.600 $\pm$ 0.085	0.625 $\pm$ 0.046	0.553 $\pm$ 0.072
AtpB	0.103 $\pm$ 0.021	0.114 $\pm$ 0.023	0.137 $\pm$ 0.016	0.116 $\pm$ 0.057
NifH	0.165 $\pm$ 0.017	0.163 $\pm$ 0.032	0.255 $\pm$ 0.060	0.173 $\pm$ 0.025
GlnA	0.111 $\pm$ 0.012	0.097 $\pm$ 0.012	0.129 $\pm$ 0.007	0.107 $\pm$ 0.014
5 h after the onset of light				
PsbA	0.088 $\pm$ 0.005	0.075 $\pm$ 0.012	0.068 $\pm$ 0.018	0.056 $\pm$ 0.017
PsaC	0.123 $\pm$ 0.019	0.120 $\pm$ 0.010	0.087 $\pm$ 0.008	0.084 $\pm$ 0.005
RbcL	0.683 $\pm$ 0.075	0.709 $\pm$ 0.065	0.563 $\pm$ 0.048	0.529 $\pm$ 0.054
AtpB	0.214 $\pm$ 0.034	0.142 $\pm$ 0.010	0.159 $\pm$ 0.061	0.128 $\pm$ 0.035
NifH	0.256 $\pm$ 0.009	0.270 $\pm$ 0.057	0.349 $\pm$ 0.035	0.167 $\pm$ 0.025
GlnA	0.120 $\pm$ 0.000	0.090 $\pm$ 0.024	0.139 $\pm$ 0.013	0.108 $\pm$ 0.004
Average of both time points				
PsbA	0.085 $\pm$ 0.015	0.070 $\pm$ 0.017	0.064 $\pm$ 0.014	0.048 $\pm$ 0.014
PsaC	0.118 $\pm$ 0.015	0.128 $\pm$ 0.013	0.092 $\pm$ 0.011	0.087 $\pm$ 0.010
RbcL	0.593 $\pm$ 0.115	0.655 $\pm$ 0.091	0.594 $\pm$ 0.054	0.541 $\pm$ 0.059
AtpB	0.158 $\pm$ 0.079	0.128 $\pm$ 0.019	0.148 $\pm$ 0.016	0.122 $\pm$ 0.008
NifH	0.201 $\pm$ 0.051	0.217 $\pm$ 0.072	0.302 $\pm$ 0.068	0.169 $\pm$ 0.033
GlnA	0.116 $\pm$ 0.006	0.093 $\pm$ 0.005	0.134 $\pm$ 0.007	0.108 $\pm$ 0.000

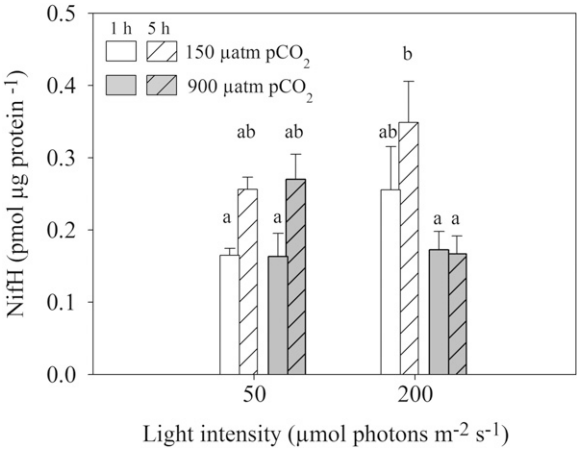

Figure 2. Changes in the amount of the nitrogenase Fe protein, NifH (pmol μg protein^{-1}), in response to different light (50 and 200 μmol photons m^{-2} s^{-1}) and pCO_2 (150 and 900 μatm) levels. White bars represent 150 μatm pCO_2, and gray bars represent 900 μatm CO_2. Plain and striped bars represent values measured at 1 and 5 h after the onset of light, respectively. Error bars indicate $\pm$1 SD (n = 3). Significance between groups was determined by one-way ANOVA ($P < 0.05$) followed by a Scheffe posthoc test. Different letters represent significant differences between groups.

pendency was observed only for the low-light acclimations (Table I).

Abundance of Photosynthetic Proteins

Both pCO_2 and light affected the abundance of PsbA (D1 protein of PSII; Fig. 3A; Table I). Elevated pCO_2 lowered the amount of PsbA at both light intensities. PsbA amounts decreased significantly from the low-pCO_2/low-light acclimation (0.085 $\pm$ 0.015 pmol μg protein^{-1}) to the high-pCO_2/high-light acclimation (0.048 $\pm$ 0.014 pmol μg protein^{-1}).

Light was the only variable responsible for changes in the amount of PsaC, a core subunit of PSI. At low light, the average PsaC amount (pmol μg protein^{-1}) for both low- and high-pCO_2 acclimations was approximately 140% higher than its average amount at high light (Fig. 3B; Table I). PsaC amount was significantly higher for high-pCO_2/low-light acclimation (0.128 $\pm$ 0.013 pmol μg protein^{-1}) in comparison with the high-pCO_2/high-light acclimation (0.087 $\pm$ 0.010 pmol μg protein^{-1}).

The relative abundance of the two photosystems, PSI:PSII, was determined using two methods: calculating the ratio of PsaC:PsbA protein pools (data calculated from Table I; Fig. 3C) and deconvolution of the emission spectra at 77 K (Fig. 3D). Despite the differences between the two methods, both revealed similar patterns. Light and the interaction of light and pCO_2 distinctly modulated PsaC:PsbA ratios (Fig. 3C). For the 77 K emission spectra, pCO_2 was the only influencing factor. Nevertheless, the average values from the 77 K measurements per acclimation revealed a significant increase in the PSI:PSII ratio between the low-pCO_2/low-light (2.844 $\pm$ 0.588 pmol μg protein^{-1}; Fig. 4D) and the high-pCO_2/high-light (3.895 $\pm$ 0.531 pmol μg protein^{-1}) acclimations.

The enzyme Rubisco catalyzes the first step in inorganic carbon fixation via the Calvin cycle. In our experiments, the amount of the large subunit of Rubisco (RbcL) was not affected by any of our variables (pCO_2, light, and time).

PSII Variable Chlorophyll Fluorescence

PSII variable chlorophyll fluorescence reflects changes in PSII activity (Fig. 4). pCO_2 concentrations and the interactions of light and time influenced the intrinsic (F_o) and maximal (F_m) fluorescence of PSII (Fig. 4, A and B). Nevertheless, no significant differences were found for the averages of both parameters (F_o and F_m) between all our acclimations (Fig. 4, A and B).

Both variable fluorescence ($F_v = F_m - F_o$) and photochemical quantum yield of PSII (F_v/F_m) were significantly influenced by pCO_2, light, and time (Fig. 4, C and D). F_v decreased with elevated pCO_2 at both light intensities and declined at 5 h after the onset of light in all acclimations (excluding the high-pCO_2/low-light acclimation; Fig. 4C). The interaction of light and time also notably decreased F_v. In all our measurements, F_v/F_m decreased at 5 h after the onset of light and was affected more by light and time of day than by pCO_2 level (Fig. 4D).

Light and time of day (but not pCO_2) influenced the effective absorbance cross-section of PSII (σ_{PSII}; Fig. 4E), although all values averaged between approximately 200 to 250 Å^2. The average σ_{PSII} value was only notably different in the high-pCO_2/high-light acclimation at 5 h after the onset of light measurement, yet it was still in the 200 to 250 Å^2 range.

The reoxidation time of the Qa^-, the primary electron acceptor of PSII (τ_{Qa}), was generally longer in the dark (Fig. 5). At 1 h after the onset of light, only ambient light notably affected the Qa^- reoxidation time. During this time point, reoxidation times ranged between 500 and 1,000 μs (Fig. 5A). At 5 h after the onset of light, both acclimation irradiance (50 or 200 μmol photons m^{-2} s^{-1}) and ambient light (dark- or light-acclimated cultures) affected τ_{Qa}, with a significant interaction between them. During midday, reoxidation time of Qa^- in the dark was longer ($\tau_{Qa} > 1{,}000$ μs) for all low-light-acclimated cultures, indicating a more reduced PQ pool in the dark (Fig. 5B). At this time point, the low-pCO_2/high-light acclimation was the only acclimation for which the time for Qa^- reoxidation did not increase in the dark (Fig. 5B).

Electron Transfer in PSII

The number of open PSIIs represents the fraction of the PSII reaction centers that are available to perform photochemistry. This fraction, calculated from the

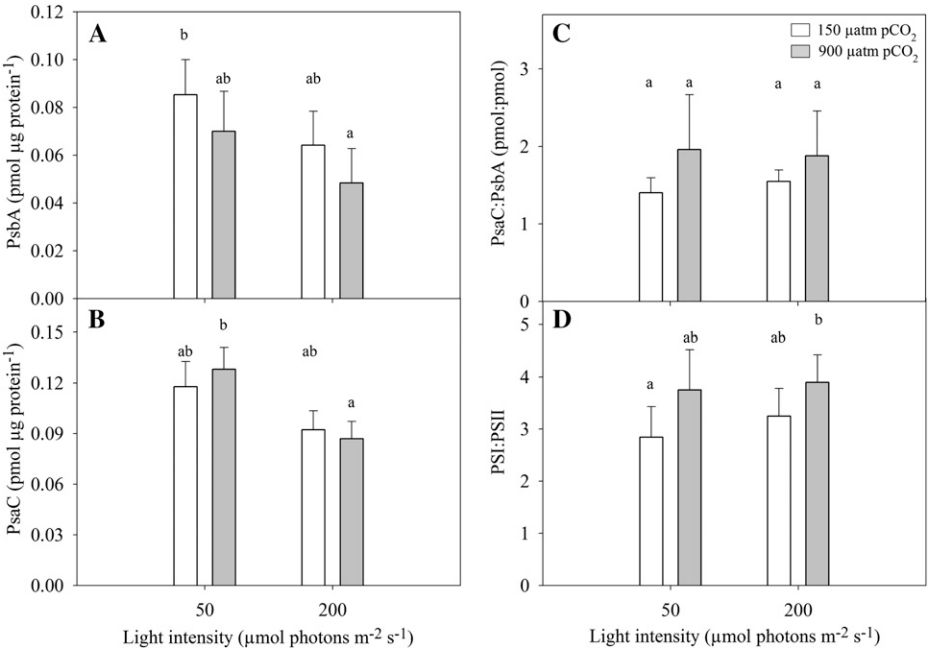

Figure 3. Changes in the average amount of photosynthetic proteins and changes in the average relative abundance of PSI and PSII in response to different light (50 and 200 μmol photons m^{-2} s^{-1}) and pCO_2 (150 and 900 μatm) levels. A, PSII protein, PsbA (D1; pmol μg $protein^{-1}$; $n = 6$). B, PSI protein, PsaC (pmol μg $protein^{-1}$; $n = 6$). C and D, Average relative abundance of the photosystems. C, Based on the quantification of the protein subcomplexes PsaC:PsbA (pmol:pmol; $n = 6$). D, Based on 77 K emission spectra ($n = 7$–10). White bars represent 150 μatm pCO_2, and gray bars represent 900 μatm pCO_2. Error bars indicate ± 1 SD. Significance between groups was determined by one-way ANOVA ($P < 0.05$) followed by a Scheffe posthoc test. Different letters represent significant differences between groups.

fluorescence parameters measured at a given growth irradiance and in the dark (Eq. 1), was not influenced by any of the tested variables and ranged from 0.801 ± 0.127 for low pCO_2/low light to 0.669 ± 0.386 at high pCO_2/high light (data not shown).

pCO_2, light, and their interaction influenced the electron transfer rate of PSII (ETR; Eq. 2; Fig. 6). Generally, the ETR decreased as pCO_2 increased. This trend was statistically significant only for the high-light acclimations.

DISCUSSION

Our study provides information on the responses of metabolic processes in *Trichodesmium* IMS101 to changes in pCO_2 (150 and 900 μatm) and light (50 and 200 μmol photons m^{-2} s^{-1}). The first part of this study (Kranz et al., 2010) focused on quantifying fluxes of cellular O_2 evolution, light-dependent O_2 uptake, nitrogen acquisition, and the uptake and fixation of inorganic carbon. Here, we examined the activity of PSII and changes in protein amounts of major photosynthetic and nitrogen metabolism complexes (Fig. 1). One of the most notable results we observed was the uncoupling between protein amounts and their functional activities. In fact, the high-pCO_2/high-light acclimation revealed that for some proteins, the highest rates (Kranz et al., 2010) were often observed at the lowest protein amounts (Table I; Fig. 7).

Nitrogen Fixation

In view of the integrated N_2 fixation rates (Kranz et al., 2010), smaller protein pools yielded higher N_2 fixation rates when acclimated to high pCO_2 for both light intensities. At high light, elevated pCO_2 increased the integrated diel N_2 fixation rates by 112% while being supported by only 50% to 66% of the NifH amount. At low light, the pCO_2 effect on N_2 fixation rates was even more pronounced, allowing a 200% increase in the diel N_2 fixation with no change in protein amounts between pCO_2 acclimations (Figs. 2 and 7; Table I; Kranz et al., 2010).

Acclimations to different pCO_2 and light intensities also changed the diurnal pattern of N_2 fixation (Kranz et al., 2010). Both high-light acclimations demonstrated the typical maximal N_2 fixation rates at midday (Berman-Frank et al., 2001), while the low-light acclimations resulted in an earlier fixation peak (Kranz et al., 2010). Yet, NifH amounts increased at midday for all acclimations except the high pCO_2/high light (Fig. 2; Chen et al., 1998). At high pCO_2/high light, NifH amounts were similar at 1 and 5 h after the onset of light and were as low as the early morning values of all other acclimations (Fig. 2), corroborating earlier observations (Levitan et al., 2010).

These results emphasize that environmental conditions regulate nitrogenase activity. In *Trichodesmium*, two forms of nitrogenase Fe protein (NifH) of low and high molecular mass are known (Zehr et al., 1993). The high-molecular-mass form appears when no N_2 fixation occurs, while the low-molecular-mass form appears at the time of N_2 fixation (Zehr et al., 1993). The switch between forms is considered a posttranslational regulation caused by a reversible ADP ribosylation of the NifH (Zehr et al., 1993; Chen et al., 1998). In *Azospirillum brasilense* and *Azotobacter chroococcum*, posttranslational modifications of NifH occur when the cells are shifted to anaerobic conditions or upon the addition of NH_4^+ (Zhang et al., 1993; Munoz-Centeno et al., 1996). The same mechanism, controlled

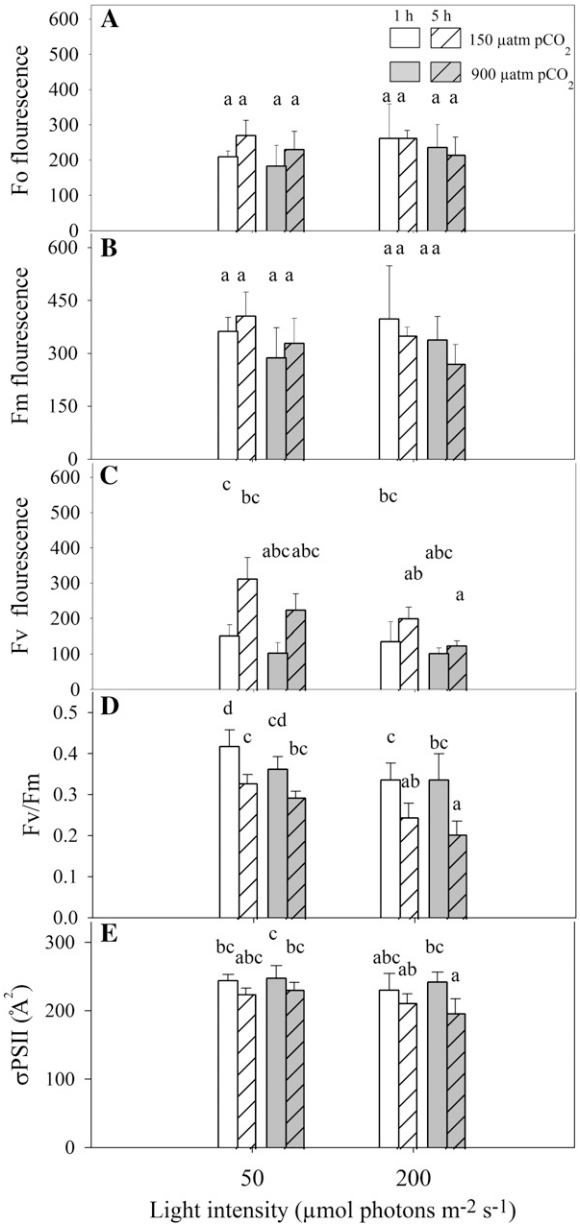

Figure 4. The influence of different light (50 and 200 μmol photons m^{-2} s^{-1}) and pCO_2 (150 and 900 μatm) levels on PSII parameters based on PSII fluorescence. A, Intrinsic fluorescence (F_o; a.u.). B, Maximal fluorescence (F_m; a.u.). C, Variable fluorescence ($F_v = F_m - F_o$; a.u.). D, PSII photochemical quantum yield (F_v/F_m). E, The effective absorbance cross-section of PSII (σ_{PSII}; $Å^2$). White bars represent 150 μatm pCO_2, and gray bars represent 900 μatm pCO_2. Plain and striped bars represent values at 1 and 5 h after the onset of light, respectively. Error bars indicate ± 1 SD ($n = 9$). Significance between groups was determined by one-way ANOVA ($P < 0.05$) followed by a Scheffe posthoc test. Different letters represent significant differences between groups.

by NH_4^+ availability and light level, was observed for the phototrophic purple bacterium *Rhodobacter capsulatus* (Masepohl et al., 2002). Therefore, posttranslational regulation could be one mechanism enabling changes in the diurnal pattern of the N_2 fixation rates in *Trichodesmium* (Levitan et al., 2010).

Photosynthetic Proteins and Acclimation Strategies

The influence of light energy on photosynthesis and photosynthetic proteins is well known. Similar to the NifH, the PsbA amounts (D1 protein, a core subunit of PSII) decreased with elevation of both pCO_2 and light (Fig. 3A) while supporting increased O_2 evolution rates detected at high light (Fig. 7; Kranz et al., 2010). This is in agreement with several studies showing that acclimation of phytoplankton to high irradiance can reduce the number of photosynthetic units and also result in higher maximal photosynthetic rates per unit of chlorophyll (Sukenik et al., 1987, and refs. therein; Behrenfeld et al., 1998; MacKenzie et al., 2004).

PSII fluorescence measurements can be used to understand the efficiency and kinetics of electron transport in the thylakoid membrane (Fig. 1). Our results show no significant change in the maximal photochemical quantum yield of PSII (F_v/F_m) under different pCO_2 levels (Fig. 4C), corroborating previ-

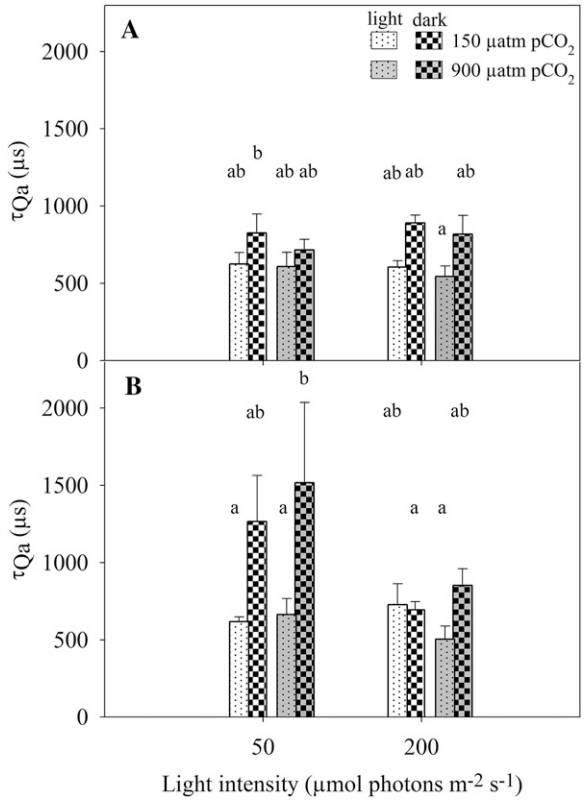

Figure 5. The influence of different light (50 and 200 μmol photons m^{-2} s^{-1}) and pCO_2 (150 and 900 μatm) levels on the relaxation time of the Qa^- (μs). A, At 1 h after the onset of light. B, At 5 h after light. White bars represent 150 μatm pCO_2, and gray bars represent 900 μatm pCO_2. Dotted bars represent values measured during ambient illumination at the growth conditions, and checkered bars represent values measured after acclimation to dark. Error bars indicate ± 1 SD ($n = 3$). Significance between groups was determined by one-way ANOVA ($P < 0.05$) followed by a Scheffe posthoc test. Different letters represent significant differences between groups.

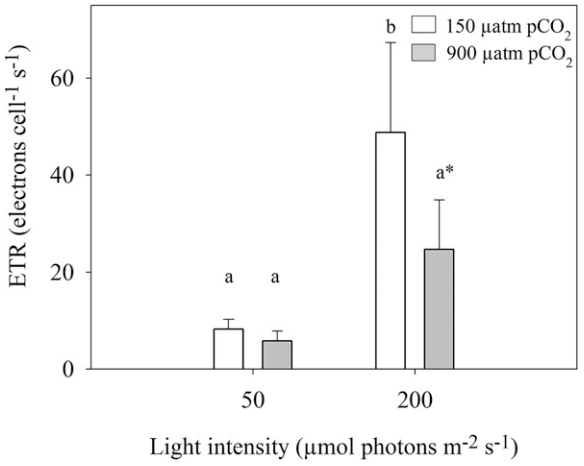

Figure 6. The influence of different light (50 and 200 μmol photons m^{-2} s^{-1}) and pCO_2 (150 and 900 μatm) levels on PSII electron transfer rate (ETR; electrons $cell^{-1}$ s^{-1}). White bars represent 150 μatm pCO_2, and gray bars represent 900 μatm pCO_2. Error bars indicate ± 1 SD (n = 6). Significance between groups was determined by one-way ANOVA ($P < 0.05$) followed by a Scheffe posthoc test. Different letters represent significant differences between groups; the asterisk represents a value that is significantly different from both low-light values according to t test ($P < 0.01$).

ously published data (Levitan et al., 2007). Higher irradiance caused a significant decrease in the F_v/F_m of *Trichodesmium* cultures that was paralleled by a decline in PsbA amounts (Figs. 3A and 4C). Thus, irradiance, and not pCO_2, influences the quantum yield of PSII.

Irradiance was also the only factor affecting the amounts of the PSI core protein PsaC (Fig. 3B). At high light, PsaC amounts decreased, as observed for the cyanobacterium *Synechococcus elongatus* under replete inorganic carbon concentrations (MacKenzie et al., 2004). Lower PsaC abundance may result from a parallel decrease of PSII amount and/or from translational or posttranslational regulation of PSI due to changes in the redox status of the electron transport components (Fujita, 1997).

Acclimation of cyanobacteria to different light intensities is often mediated by changes in the stoichiometry of the two photosystems, PSI:PSII (Fig. 3, C and D; Fujita, 1997; MacKenzie et al., 2004), and in phycobilisome assembly. Flexible photosystem stoichiometry is also essential for controlling the production of ATP and reductants (Fujita, 1997). PSI:PSII ratios were higher at elevated pCO_2 and high light (Fig. 3, C and D). Higher PSI:PSII ratios may enable a higher electron flow through linear photosynthetic electron transport. This can increase electron flux toward ferredoxin reduction and enable enhanced N_2 fixation and/or NADPH production. Alternatively, the higher PSI may support the activation of the NDH-1_4 as a CO_2 uptake mechanism (Kranz et al., 2010) and promote higher ATP production (Figs. 1 and 7).

Photosynthetically generated reductants are used in the Calvin cycle to reduce inorganic carbon to carbohydrates. Although key enzymes in the Calvin cycle, including Rubisco, are "switched on" with light, Rubisco's transcripts and efficiency are known to be light insensitive (Falkowski and Raven, 2007). In our experiment, neither pCO_2 nor light influenced RbcL amounts for all the acclimations (Table I). Nevertheless, RbcL:PsbA ratios were higher when increasing pCO_2 and/or light (Table I). When transferring low-light-acclimated cultures to high light, O_2 evolution and inorganic carbon fixation rates were the same as for high-light-acclimated cultures, regardless of the RbcL:PsbA ratio (Kranz et al., 2010). This indicates that light-saturated photochemistry in *Trichodesmium* is limited by carbon fixation and not by electron transfer from PSII (Sukenik et al., 1987; Falkowski, 1992).

Our results exhibit constant σ_{PSII} (excited by blue light) values of approximately 200 to 250 $Å^2$, which correspond to the typically low σ_{PSII} found in cyanobacteria (Suggett et al., 2006) and with previously measured σ_{PSII} of *Trichodesmium* (Shi et al., 2007; Küpper et al., 2008; I. Berman-Frank and O. Levitan, unpublished data; Fig. 4E). Maintaining a relatively constant σ_{PSII} while changing the number (n) of PSII reaction centers (represented by the amount of PsbA) characterizes a strategy termed "n-type" light acclimation (Falkowski and Owens, 1980). This strategy is also correlated with changes in RbcL:PsbA ratio (Table I), as described for natural populations of *Trichodesmium* in the Gulf of Mexico (Brown et al., 2008). A strategy of keeping a small σ_{PSII} while changing the amount of reaction center protein complexes was postulated for natural phytoplankton populations of the upper water column as a means to manage PSII in case of photodamage (Behrenfeld et al., 1998). Since *Trichodesmium* species are often found near the surface, an n-type acclimation is advantageous.

We suggest that the observed changes in PsbA and PsaC are not a consequence of photosynthetic stress (limitation) but rather an acclimation strategy. Under elevated pCO_2 and light, the ability of *Trichodesmium* to reduce its investment in the synthesis of expensive proteins (PsbA, PsaC) while increasing its PSI:PSII ratio allows for increased N_2 fixation, improved carbon uptake, and enhanced growth (Fig. 7).

Energy Generation and Photosynthetic Electron Flow

In our experiments, the half-time of Qa^- reoxidation, τ_{Qa}, under actinic irradiances was found to be approximately 500 μs, matching previously published values for phytoplankton (Falkowski et al., 1986; Kolber et al., 1998; Lardans et al., 1998). The difference between the reoxidation time in the dark- versus light-acclimated cultures indicates the contribution of processes that reduce the PQ pool in the dark, such as the activation of succinate dehydrogenase and NADPH dehydrogenase (Fig. 1; Cooley et al., 2000; Cooley and Vermaas, 2001). At 5 h after the onset of light, this reduction of PQ in the dark was higher for the low-light-acclimated cultures. The redox state of the PQ

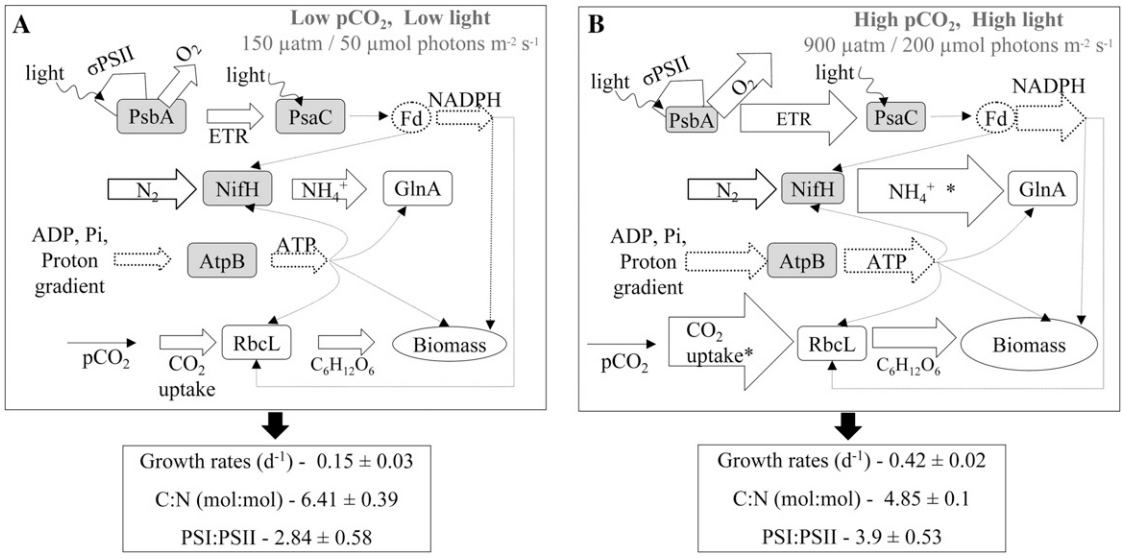

Figure 7. A schematic comparison of the changes taking place in *Trichodesmium* IMS101 when acclimated to 150 μatm/50 μmol photons m^{-2} s^{-1} and 900 μatm/200 μmol photons m^{-2} s^{-1}. A, Fluxes, protein pools, and σ_{PSII} under low pCO_2 and low light (150 μatm/50 μmol photons m^{-2} s^{-1}). B, Fluxes, protein pools, and σ_{PSII} under high pCO_2 and high light (900 μatm/200 μmol photons m^{-2} s^{-1}). Amounts of protein complexes are taken as average values from Table I, average of both time points. PSI:PSII ratios are the values corresponding to Figure 5B (77 K measurements). Fluxes of carbon fixation, CO_2 uptake, N_2 fixation, and O_2 evolution, as well as growth rates and carbon-nitrogen ratios, are taken from Kranz et al. (2010). The differences between protein pool sizes and fluxes are represented proportionally by changes in the area of the protein subunits measured and the arrow size of measured fluxes. A shows baseline amounts, and changes in B are relative to those in A. Changes in N_2 fixation and CO_2 uptake rates (marked with asterisks [B]) are not presented proportionally as the changes were too big to plot. Protein subunits shaded gray represent proteins that we suggest to be posttranslationally regulated by pCO_2 and light. Dotted lines and shapes represent fluxes that were not measured.

pool regulates biosynthesis and the function of photosynthetic and respiratory complexes (Fujita et al., 1987; Pfannschmidt et al., 2001) and can be connected to the observed changes in photosynthetic protein amount and activity (Fig. 7; Kranz et al., 2010).

The efficiency of the photosynthetic ETR is affected by the redox state of the electron acceptors such as Qa and the PQ pool (Suggett et al., 2006). We observed changes in ETR in the different acclimations (Fig. 6) while maintaining an equal fraction of open PSII (data not shown). ETR flexibility could account for the cells' ability to rapidly adjust to differing light regimes. This was observed when measuring the immediate increase in O_2 evolution rates for low-light-acclimated cells that were transferred to high-light conditions (Kranz et al., 2010). This strategy may serve as a shunting valve for dissipating excess energy (Campbell et al., 1998; MacKenzie et al., 2004), which would be necessary for natural phytoplankton populations (Behrenfeld et al., 1998), including *Trichodesmium* species that form huge surface blooms in the high-light environments of the tropical oceans.

Discrepancies between ETR and O_2 evolution rates (Fig. 6; Kranz et al., 2010) may be related to the activity of the Mehler reaction, as both were observed only for the low-pCO_2/high-light acclimation. When there is not enough oxidized ferredoxin/$NADP^+$ acting as photosynthetic electron acceptors, O_2 can be used as an alternative electron acceptor in the Mehler reaction (Kana, 1992). Both low-light acclimations exhibited Mehler activity immediately when transferred from low to high light (Kranz et al., 2010). This suggests that the Mehler reaction, acting as an energy-dissipating mechanism, decouples ETR from photosynthetic O_2 evolution and carbon fixation (Kranz et al., 2010), in agreement with previous reports for cyanobacteria acclimated to high light (Kana, 1992; Suggett et al., 2006).

Neither pCO_2 nor light significantly influenced the amount of AtpB (CF_1 subunit of ATP synthase), the major protein responsible for cellular energy production (Table I). ATP production depends on a cross-membrane proton gradient of the thylakoid membrane and can be enhanced by faster respiration and/or photosynthetic electron transfer rates (Fig. 1; Falkowski and Raven, 2007). ATP synthase activity is controlled at the protein level and by the redox state of the electron transport chain, allowing up to 1 order of magnitude increase in catalytic activity (Allen et al., 1995; Falkowski and Raven, 2007, and refs. therein). Therefore, at elevated pCO_2 and light, enhanced ETR (Fig. 6) combined with high PSI:PSII ratios (Fig. 3, C and D), allowing more cyclic electron flow around PSI and high internal inorganic carbon cycling (Kranz et al., 2010), may support higher ATP production for the same amount of AtpB (Fig. 7).

Low-pCO_2/High-Light Acclimation

This acclimation revealed unique characteristics, which can provide a way to discriminate the contribution of pCO_2 and light to the cells' metabolic regulation and electron flow. This was the only acclimation for which NifH and GlnA amounts were notably high (Fig. 2; Table I) and light-dependent O_2 uptake (Mehler reaction) was detected (Kranz et al., 2010). In addition, light and dark Qa^- reoxidation times were the same during midday (Fig. 5), probably as a result of a more reduced PQ pool in the light (Fig. 1). The reduced PQ pool can be a consequence of the high ETR detected for this acclimation (Fig. 6), thereby leading to electron transport toward the Mehler reaction (Kranz et al., 2010).

All of the above suggest that the combination of low pCO_2 with high light may decouple processes that are primarily activated by light. Such processes could meet their metabolic balance by using environmental regulatory signals like pCO_2. This acclimation, low pCO_2/high light, may simulate natural conditions that can occur during massive surface blooms, frequently observed for *Trichodesmium* populations in the tropical oceans (Capone and Subramaniam, 2005).

CONCLUSION

Previous studies suggest that *Trichodesmium* species will thrive in the future acidified (Barcelos é Ramos et al., 2007; Hutchins et al., 2007, 2010; Levitan et al., 2007, 2010; Kranz et al., 2009) and warmer (Hutchins et al., 2007; Levitan et al., 2010) oceans. In this study, we show that in *Trichodesmium*, elevated pCO_2 and light lead to increased metabolic fluxes that correspond to lower amounts of several key proteins (Fig. 7). Reducing energetic and resource requirements for protein synthesis can divert this "excess" to N_2 fixation and growth. We suggest that the flexible metabolism and photosynthetic protein stoichiometry in *Trichodesmium* is mediated by changes in the redox state of the PQ pool and by posttranslational regulation of key proteins. This strategy maintains balanced growth and retains the known range for *Trichodesmium* carbon-nitrogen ratios. Changes in the CO_2-concentrating mechanism operation under high pCO_2 (Kranz et al., 2009, 2010) can provide further energy and resources to support higher metabolic throughput and growth (Fig. 7). Our results imply that the above acclimation behavior would enable this ancient cyanobacterium to adapt to the projected changing conditions of pCO_2 and light. This could facilitate bloom expansion, increasing the contribution of *Trichodesmium* species to the carbon and nitrogen biogeochemical cycles.

MATERIALS AND METHODS

Culture Conditions and Carbonate Chemistry

Semicontinuous dilute batch cultures of *Trichodesmium* IMS101 (originally isolated by Prufert-Bebout et al. [1993]) were grown at 25°C in 0.2-μm-filtered unbuffered nitrogen-free artificial seawater (YBCII medium; Chen et al., 1996). Cultures were grown as single filaments in 1-L cylindrical glass flasks (diameter of 7 cm) in pCO_2-preacclimated YCBII medium. The light regime was a 12/12-h light/dark cycle at two different light intensities, 50 μmol photons m^{-2} s^{-1} (low light) and 200 μmol photons m^{-2} s^{-1} (high light). The 200 μmol photons m^{-2} s^{-1} was chosen for saturating but not photodamaging irradiance according to Breitbarth et al. (2008). Light was supplied using white fluorescent bulbs (Osram; BIOLUX). Cultures were continuously bubbled with air containing different pCO_2 values of 150 and 900 μatm. The gentle bubbling was sufficient to prevent the formation of aggregates but did not cause high turbulence that could harm the integrity of the filaments. CO_2 gas mixtures were generated using gas-mixing pumps (Digamix 5KA18/8-F and 5KA36/8-F; Woesthoff), CO_2-free air (Nitrox CO_2RP280; Domnick Hunter), and pure CO_2 (Air Liquide Deutschland). Experiments were done using at least three independent replicates.

Cultures were acclimated to experimental conditions at least 2 months prior to measurements. While species acclimate differently to changes in growth conditions, it is generally assumed that more than 10 generations are sufficient (MacIntyre and Cullen, 2005). Cultures were unialgal, and at exponential growth bacterial biomass was not observed under light microscopy (×400 magnification).

Use of dilute batch cultures with experiments performed at the midexponential growth of the cells retained the carbonate chemistry constant. The pH was 8.57 ± 0.03 and 7.94 ± 0.03 for the low- and high-pCO_2 acclimations, respectively, and was determined every morning using a pH/ion meter (model 713 pH meter; Metrohm). Cultures in which the pH had shifted (pH shift > 0.06) in comparison with a reference (cell-free YBCII at the respective pCO_2 levels) were excluded from further analysis. The carbonate system was calculated from total alkalinity, pH, temperature, salinity, and phosphate using CO2Sys (Lewis and Wallace, 1998). Carbonate chemistry parameters for the respective CO_2 treatments are supplied by Kranz et al. (2010).

Sample Collection for Proteins

Samples of *Trichodesmium* IMS101 were collected 1 and 5 h after the onset of light by gentle filtration on 5-μm pore size polycarbonate filters (13 mm diameter; Osmonics) in the dark. Filtration volumes were 25 to 70 mL (depending on acclimation and culture biomass) and lasted approximately 1 to 3 min. Filters were placed in sterile DNase- and RNase-free centrifuge tubes, directly frozen with liquid nitrogen, and subsequently stored at −80°C.

Total Protein Extraction and Quantification

Trichodesmium filters were resuspended in 250 μL of 1× denaturing extraction buffer containing 140 mM Tris base, 105 mM Tris-HCl, 0.5 mM EDTA, 2% lithium dodecyl sulfate, 10% glycerol, and 0.1 mg mL^{-1} PefaBloc SC (AEBSF) protease inhibitor (Roche). Samples were sonicated until thawed using a Fisher Scientific model 100 sonic dismembrator with a microtip attachment at a setting of 30%. To avoid overheating, samples were then refrozen immediately in liquid N_2. Two cycles of freezing followed by thawing by sonication yielded maximal protein extraction with minimal degradation of representative membranes and soluble proteins (Brown et al., 2008). Following disruption, samples were centrifuged for 3 min at 10,000*g* to remove insoluble material and unbroken cells. The total protein concentration was measured with a modified Lowry assay (Bio-Rad) using bovine γ-globulin as a comparative protein standard.

Target Protein Quantification

Key protein quantification was performed using standards (AgriSera) and followed the procedure described by Brown et al. (2008) and Levitan et al. (2010). Primary antibodies (AgriSera) were used at a dilution of 1:40,000 in 2% ECL advance blocking reagent in Tris-buffered saline plus Tween 20 for NifH (Fe protein of nitrogenase), GlnA (a subunit of Gln synthetase), PsbA (D1 protein of PSII), PsaC (core subunit of PSI), AtpB (the CF_1 subunit of ATP synthase), and RbcL (the large subunit of Rubisco). Blots were incubated for 1 h with horseradish peroxidase-conjugated rabbit anti-chicken secondary antibody (Abcam) for the NifH, GlnA, AtpB, and RbcL primary antibodies and with horseradish peroxidase-conjugated chicken anti-rabbit secondary antibody (Abcam) for the PsbA and PsaC primary antibodies and diluted 1:40,000 in 2% ECL Advance blocking reagent in Tris-buffered saline plus Tween 20. Blots were developed with ECL Advance detection reagent

(Amersham Biosciences, GE Healthcare) using a CCD imager (DNR; M-ChemiBIS). For estimating the amounts of protein in experimental samples, protein levels on immunoblots were quantified using Quantity One software (Bio-Rad) and calculated from standard curves (for each blot, after Brown et al. [2008]).

PSII Variable Chlorophyll Fluorescence

PSII fluorescence parameters of *Trichodesmium* IMS101 were measured twice a day, 1 and 5 h after the onset of light, using the Fluorescence Induction and Relaxation System (FIRe; Satlantic; Falkowski et al., 2004). This instrument is based on the same biophysical principles as the fast repetition rate fluorometer (Kolber et al., 1998), with light-emitting diode excitation at 450 ± 30 nm and emission detected using a greater than 678-nm long-pass filter.

Fluorescence parameters were as follows: F_o, intrinsic fluorescence (arbitrary units [a.u.]); F_m, maximal fluorescence (a.u.); F_v, variable fluorescence ($F_v = F_m - F_o$ [a.u.]); F_v/F_m, PSII photochemical quantum yield; σ_{PSII}, effective absorbance cross-section of PSII (Å^2); and τ_{Qa}, relaxation time of the Qa^- (μs). All parameters were measured after acclimation to dark (15 min), so that all PSII reaction centers are photochemically oxidized. Additional measurements were performed under growth irradiance (50 or 200 μmol photons m^{-2} s^{-1}) with an ambient light source (Satlantic). Blanks were prepared by filtering each sample using 0.2-μm sterile Minisert filters (Sartorius), and blank traces were subtracted for each measurement.

For the F_o, F_m, F_v, F_v/F_m, and σ_{PSII} parameters, data analysis was performed using a Matlab code (http://sourceforge.net/projects/fireworx) written by Audrey Burnett from John Cullen's laboratory (Department of Oceanography, Dalhousie University, Halifax, Canada) in coordination with Satlantic. F_o and F_m values were normalized to the culture chlorophyll values (Campbell et al., 1998). For the τ_{Qa} analysis, we used the FIRePro software provided by Satlantic.

Calculation of Open PSII Reaction Centers and PSII Electron Transfer Rate

The number of open PSII reaction centers ($PSII_{OPEN}$) and electron transfer rate of PSII (ETR_{PSII}) were calculated using values from the photosynthetic fluorescence analysis and the amount of PsbA per cell calculated from quantitative western blots. $PSII_{OPEN}$ was calculated according to Equation 1 (Kooten and Snel, 1990; MacKenzie et al., 2004):

$$PSII_{OPEN} = (F'_m - F_s)/(F'_m - F_o) \quad (1)$$

where F_m' is the maximum fluorescence in light-acclimated cultures, F_s is the steady-state fluorescence level in the respective growth irradiance, and F_o is the minimum fluorescence level measured in the dark (Krause and Weis, 1991).

ETR_{PSII} was calculated according to Equation 2 (MacKenzie et al., 2005; modified from Falkowski and Raven, 1997):

$$ETR_{PSII} = \left[E \times PSII_{OPEN} \times \sigma_{PSII} \times (\text{PSII cell}^{-1})\right] \quad (2)$$

where E is the photon flux density of the illumination, $PSII_{OPEN}$ is the ratio of the photochemically reduced (open) PSII reaction centers, σ_{PSII} is the effective absorbance cross-section of PSII, and PSII cell^{-1} is the number of PSII reaction centers in a cell. Since cultures were growing under acclimated, nonphotoinhibitory conditions, PSII cell^{-1} was estimated according to the number of D1 (PsbA) protein subunits to reflect the number of PSII reaction centers (Burns et al., 2006).

Relative Abundance of Photosystems

The relative abundance of the two photosystems (PSI and PSII) was determined from emission spectra at 77 K. Samples were collected on a 13-mm glass fiber filter placed on a sample holder in a quartz dewar filled with liquid nitrogen. The spectra were determined using a portable low-temperature spectrometer using 450-nm excitation (Prášil et al., 2009), and the resulting peaks were analyzed with PeakFit 4 software (Systat). Peaks with maxima in the 680- to 695-nm regions were assigned to PSII, and peaks with maxima in the 710- to 730-nm regions were assigned to PSI. Samples were taken from each treatment during 1 and 5 h after the onset of light. The number of independent replicates was seven to 10 for each acclimation.

Statistical Analysis

All the results presented in this report were checked using several statistical tests. Protein abundance and most fluorescence data were analyzed by three-way ANOVA with interactions (pCO_2, light, and time; $P < 0.05$). Analysis of Qa^- reoxidation was also done using three-way ANOVA with interactions (pCO_2, acclimation irradiance, and ambient light; $P < 0.05$). Interactions between the variables from the three-way ANOVA are stated here only when significant ($P < 0.05$). To find significant differences between the average values of four to eight groups (treatments and time of day), we used one-way ANOVA ($P < 0.05$) followed by a Scheffe posthoc test. In the figures, different letters represent significant differences determined according to the Scheffe posthoc tests, with increasing average values from a to d (a is assigned for the lowest average value). Values denoted by two letters or more (e.g. ab) represent average values that are not significantly different from the main groups represented by these letters. For verifying significant differences between the different pCO_2 and light conditions, we used t tests for independent variables ($P < 0.05$ or $P < 0.01$). All data in the figures are presented as average values of at least three independent replicates with ±1 SD. Numbers of independent replicates (n = 3–10) are presented for each figure in the figure legend.

ACKNOWLEDGMENTS

We thank Mr. Klaus-Uwe Richter from the Alfred Wegener Institute for Polar and Marine Research for technical support during the experiments. We thank Dr. Chris M. Brown from the Institute of Marine and Coastal Sciences, Rutgers University, for his advice regarding all protein work. We also thank Dr. Noga Stambler from Bar Ilan University and Prof. Douglas Campbell from Mount Allison University for their criticism and advice. Statistical analysis was performed with help from Dr. Rachel S. Levy-Drummer from the Mina and Everard Goodman Faculty of Life Sciences, Bar Ilan University.

Received May 15, 2010; accepted July 11, 2010; published July 12, 2010.

LITERATURE CITED

Allen JF, Alexciev K, Hakansson G (1995) Photosynthesis: regulation by redox signaling. Curr Biol **5:** 869–872

Barcelos é Ramos J, Biswas H, Schulz K, LaRoche J, Riebesell U (2007) Effect of rising atmospheric carbon dioxide on the marine nitrogen fixer *Trichodesmium*. Global Biogeochem Cycles **21:** 1–6

Behrenfeld MJ, Prášil O, Kolber ZS, Babin M, Falkowski PG (1998) Compensatory changes in photosystem II electron turnover rates protect photosynthesis from photoinhibition. Photosynth Res **58:** 259–268

Bergman B, Gallon JR, Rai AN, Stal LJ (1997) N_2 fixation by non-heterocystous cyanobacteria. FEMS Microbiol Rev **19:** 139–185

Berman-Frank I, Lundgren P, Chen YB, Kupper H, Kolber Z, Bergman B, Falkowski P (2001) Segregation of nitrogen fixation and oxygenic photosynthesis in the marine cyanobacterium *Trichodesmium*. Science **294:** 1534–1537

Breitbarth E, Wohlers J, Kläs J, LaRoche J, Peeken I (2008) Nitrogen fixation and growth rates of *Trichodesmium* IMS-101 as a function of light intensity. Mar Ecol Prog Ser **359:** 25–36

Brown CM, MacKinnon JD, Cockshutt AM, Villareal TA, Campbell D (2008) Flux capacities and acclimation costs in *Trichodesmium* from the Gulf of Mexico. Mar Biol **154:** 413–422

Burns RA, MacKenzie DB, Campbell D (2006) Inorganic carbon repletion constrains steady-state light acclimation in the cyanobacteria *Synechococcus elongatus*. J Phycol **42:** 610–621

Campbell D, Hurry V, Clarke AK, Gustafsson P, Oquist G (1998) Chlorophyll fluorescence analysis of cyanobacterial photosynthesis and acclimation. Microbiol Mol Biol Rev **62:** 667–683

Capone DG, Subramaniam A (2005) Seeing microbes from space: remote sensing is now a critical resource for tracking marine microbial ecosys-

tem dynamics and their impact on global biogeochemical cycles. ASM News **71:** 179–196

Carpenter EJ, Capone DG (2008) Nitrogen fixation in the marine environment. *In* Nitrogen in the Marine Environment, Ed 2. Academic Press, San Diego, pp 141–198

Chen YB, Dominic B, Mellon MT, Zehr JP (1998) Circadian rhythm of nitrogenase gene expression in the diazotrophic filamentous nonheterocystous cyanobacterium *Trichodesmium* sp strain IMS101. J Bacteriol **180:** 3598–3605

Chen YB, Zehr JP, Mellon M (1996) Growth and nitrogen fixation of the diazotrophic filamentous nonheterocystous cyanobacterium *Trichodesmium* sp IMS 101 in defined media: evidence for a circadian rhythm. J Phycol **32:** 916–923

Cooley JW, Howitt CA, Vermaas WFJ (2000) Succinate:quinol oxidoreductases in the cyanobacterium *Synechocystis* sp strain PCC 6803: presence and function in metabolism and electron transport. J Bacteriol **182:** 714–722

Cooley JW, Vermaas WFJ (2001) Succinate dehydrogenase and other respiratory pathways in thylakoid membranes of *Synechocystis* sp strain PCC 6803: capacity comparisons and physiological function. J Bacteriol **183:** 4251–4258

Doney SC (2006) Oceanography: plankton in a warmer world. Nature **444:** 695–696

Falkowski PG (1992) Phytoplankton photosynthesis in the ocean in relation to the global carbon cycle. Photosynth Res **34:** 108–108

Falkowski PG, Koblizek M, Gorbunov M, Kolber Z (2004) Development and application of variable chlorophyll fluorescence techniques in marine ecosystems. *In* G Papageorgiou, Govindjee, eds, Chlorophyll a Fluorescence: Signature of Photosynthesis. Springer, New York, pp 757–778

Falkowski PG, Owens TG (1980) Light-shade adaptation: two strategies in marine phytoplankton. Plant Physiol **66:** 592–595

Falkowski PG, Raven JA (1997) Aquatic Photosynthesis. Blackwell Science, Oxford, UK

Falkowski PG, Raven JA (2007) Aquatic Photosynthesis, Ed 2. Princeton University Press, Princeton, NJ

Falkowski PG, Wyman K, Ley AC, Mauzerall DC (1986) Relationship of steady-state photosynthesis to fluorescence in eukaryotic algae. Biochim Biophys Acta **849:** 183–192

Fujita Y (1997) A study on the dynamic features of photosystem stoichiometry: accomplishments and problems for future studies. Photosynth Res **53:** 83–93

Fujita Y, Ohki K, Murakami A (1987) Chromatic regulation of photosystem composition in the cyanobacterial photosynthetic system: kinetic relationship between change of photosystem composition and cell-proliferation. Plant Cell Physiol **28:** 227–234

Hutchins DA, Fu FX, Zhang Y, Warner ME, Portune K, Bernhardt PW, Mulholland MR (2007) CO_2 control of *Trichodesmium* N_2 fixation, photosynthesis, growth rates, and elemental ratios: implications for past, present, and future ocean biogeochemistry. Limnol Oceanogr **52:** 1293–1304

Hutchins DA, Mulholland MR, Fu FX (2010) Nutrient cycles and marine microbes in a CO_2 enriched ocean. Oceanogr Mar Biol Annu Rev **22:** 128–145

Kana TM (1992) Oxygen cycling in cyanobacteria with specific reference to oxygen protection in *Trichodesmium* spp. *In* EJ Carpenter, ed, Marine Pelagic Cyanobacteria: *Trichodesmium* and Other Diazotrophs. Kluwer Academic Publishers, Dordrecht, The Netherlands, pp 29–41

Kana TM (1993) Rapid oxygen cycling in *Trichodesmium thiebautii*. Limnol Oceanogr **38:** 18–24

Kolber Z, Prášil O, Falkowski PG (1998) Measurements of variable chlorophyll fluorescence using fast repetition rate techniques: defining methodology and experimental protocols. Biochim Biophys Acta **1367:** 88–106

Kooten O, Snel JFH (1990) The use of chlorophyll fluorescence nomenclature in plant stress physiology. Photosynth Res **25:** 147–150

Kranz S, Sültemeyer D, Richter KU, Rost B (2009) Carbon acquisition by *Trichodesmium*: the effect of pCO_2 and diurnal changes. Limnol Oceanogr **54:** 548–559

Kranz SA, Levitan O, Richter KU, Prášil O, Berman-Frank I, Rost B (2010) Combined effects of CO_2 and light on the N_2-fixing cyanobacterium *Trichodesmium* IMS101: physiological responses. Plant Physiol **154:** 334–345

Krause GH, Weis E (1991) Chlorophyll fluorescence and photosynthesis: the basics. Annu Rev Plant Physiol Plant Mol Biol **42:** 313–349

Küpper H, Setlik I, Seibert S, Prášil O, Setlikova E, Strittmatter M, Levitan O, Lohscheider J, Adamska I, Berman-Frank I (2008) Iron limitation in the marine cyanobacterium *Trichodesmium* reveals new insights into regulation of photosynthesis and nitrogen fixation. New Phytol **179:** 784–798

Lardans A, Forster B, Prášil O, Falkowski PG, Sobolev V, Edelman M, Osmond CB, Gillham NW, Boynton JE (1998) Biophysical, biochemical, and physiological characterization of Chlamydomonas reinhardtii mutants with amino acid substitutions at the Ala(251) residue in the D1 protein that result in varying levels of photosynthetic competence. J Biol Chem **273:** 11082–11091

Levitan O, Brown C, Sudhaus S, Campbell D, LaRoche J, Berman-Frank I (2010) Regulation of nitrogen metabolism in the marine diazotroph *Trichodesmium* IMS101 under varying temperatures and atmospheric CO_2 concentrations. Environ Microbiol **12:** 1899–1912

Levitan O, Rodsenberg G, Setlik I, Setlikova E, Grigel J, Klepetar J, Prášil O, Berman-Frank I (2007) Elevated CO_2 enhances nitrogen fixation and growth in the marine cyanobacterium *Trichodesmium*. Glob Change Biol **13:** 1–8

Lewis E, Wallace DWR (1998) Developed for CO_2 system calculations. ORNL/CDIAC-105. Carbon Dioxide Information Analysis Center, Oak Ridge National Laboratory, US Department of Energy, Oak Ridge, TN

Lin SJ, Henze S, Lundgren P, Bergman B, Carpenter EJ (1998) Whole-cell immunolocalization of nitrogenase in marine diazotrophic cyanobacteria, *Trichodesmium* spp. Appl Environ Microbiol **64:** 3052–3058

MacIntyre HL, Cullen JJ (2005) Using cultures to investigate the physiological ecology of microalgae. *In* RA Anderson, ed, Algal Culturing Techniques. Elsevier Academic Press, Burlington, MA, pp 287–326

MacKenzie TDB, Burns RA, Campbell D (2004) Carbon status constrains light acclimation in the cyanobacterium *Synechococcus elongatus*. Plant Physiol **136:** 3301–3312

MacKenzie TDB, Johnson JM, Campbell D (2005) Dynamics of fluxes through photosynthetic complexes in response to changing light and inorganic carbon acclimation in *Synechococcus elongatus*. Photosynth Res **85:** 341–357

Mahaffey C, Michaels AF, Capone DG (2005) The conundrum of marine N_2 fixation. Am J Sci **305:** 546–595

Masepohl B, Drepper T, Paschen A, Gross S, Pawlowski A, Raabe K, Riedel KU, Klipp W (2002) Regulation of nitrogen fixation in the phototrophic purple bacterium *Rhodobacter capsulatus*. J Mol Microbiol Biotechnol **4:** 243–248

Munoz-Centeno MC, Ruiz MT, Paneque A, Cejudo FJ (1996) Posttranslational regulation of nitrogenase activity by fixed nitrogen in *Azotobacter chroococcum*. Biochim Biophys Acta **1291:** 67–74

Pfannschmidt T, Allen JF, Oelmuller R (2001) Principles of redox control in photosynthesis gene expression. Physiol Plant **112:** 1–9

Prášil O, Bina D, Medova H, Rehakova K, Zapomelova E, Vesela J, Oren A (2009) Emission spectroscopy and kinetic fluorometry studies of phototrophic microbial communities along a salinity gradient in solar saltern evaporation ponds of Eilat, Israel. Aquat Microb Ecol **56:** 285–296

Prufert-Bebout L, Paerl HW, Lassen C (1993) Growth, nitrogen fixation, and spectral attenuation in cultivated *Trichodesmium* species. Appl Environ Microbiol **59:** 1367–1375

Shi T, Sun Y, Falkowski PG (2007) Effects of iron limitation on the expression of metabolic genes in the marine cyanobacterium *Trichodesmium erythraeum* IMS101. Environ Microbiol **9:** 2945–2956

Suggett DJ, Moore CM, Maranon E, Omachi C, Varela RA, Aiken J, Holligan PM (2006) Photosynthetic electron turnover in the tropical and subtropical Atlantic Ocean. Deep Sea Res Part II Top Stud Oceanogr **53:** 1573–1592

Sukenik A, Bennett J, Falkowski PG (1987) Light saturated photosynthesis: limitation by electron transport or carbon fixation? Biochim Biophys Acta **891:** 205–215

Zehr J, Wyman M, Miller V, Duguay L, Capone DG (1993) Modification of the Fe protein of nitrogenase in natural populations of *Trichodesmium thiebautii*. Appl Environ Microbiol **59:** 669–676

Zhang YP, Burris RH, Ludden PW, Roberts GP (1993) Posttranslational regulation of nitrogenase activity by anaerobiosis and ammonium in *Azospirillum brasilense*. J Bacteriol **175:** 6781–6788